Range Image Segmentation Using the Numerical Description of the Mean Curvature Values

Yahya Alshawabkeh*, Norbert Haala**, Dieter Fritsch**
Hashemite University, Jordan*
Institute for Photogrammetry (ifp), Universität Stuttgart, Germany**
yahya.alshawabkeh@hu.edu.de

KEY WORDS: Laser Scanner, Range Image Segmentation, Mean Curvature values, Crease-step edge, Free form objects.

ABSTRACT:
In this paper we present a new efficient edge detection algorithm for the extraction of linear features in both range and intensity image data. In the proposed algorithm the distinguished points, which will comprise the edges, depend on the spatial analysis of the numerical description of the mean curvature values. The work was motivated by the fact that the optimality of edge detectors for range images has not been considered in the literature, some algorithms are limited to synthetic range images and will totally fail in the presence of noise, others which have been tested in real range images are complicated with large numbers of parameters. As it will be demonstrated, the algorithm features computational efficiency, high accuracy in the localization of the edge points, easy implementation, and robustness against noise. The algorithm was initially developed for range image segmentation and has been extended to segment intensity images with some modifications. The generality and robustness of the algorithm is illustrated on complex scene images with different range sensors.

1. INTRODUCTION

Range images provide the fundamental contribution toward the goal of understanding 3-D shape, which is required for general-purpose object recognition and image understanding [Gachter et al, 2006]. The most significant problem in the early stages of image analysis is image segmentation, a process of partitioning of pixels in the image into meaningful parts in order to extracting important image features. Most of 3D segmentation algorithms are based on range images instead of unordered 3D point clouds [Chen & Stamos, 2007;Yu & Ferencz, 2001]. For such 2.5D raster grids neighborhood relations are available implicitly and tools from image processing can be adopted. Algorithms developed for the segmentation of intensity image have been discussed extensively in the literature. Well-known examples for the real time segmentation of intensity images are [Palmer et al, 1996; Canny, 1986]. In the other hand, ready-made solutions for range image segmentation are not available to a comparable extend [Gächter, 2005].

Typically, the researchers classify the edges in 3D image in two main categories; step (jump) edges: represents discontinuities on the surface. Crease (fold) edges: correspond to the discontinuities of the surface normals. Some researchers consider another type of edges called ridgelines edges, example of this type are the edges a long the extrema of the major axis of the cross section of an elliptical cylinder. For the intensity image, the devised segmentation algorithms usually aim to detect step edges. This is due to the natural limitation of this of this type of images as can be detected in the figure 1. Canny operator cannot detect the crease edges for the block range image obtained from Ohio State University (OSU) range image collection.

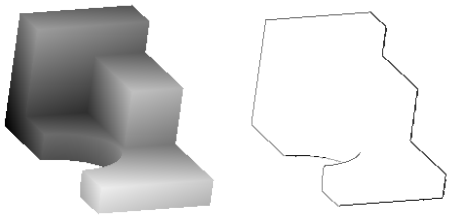

Figure 1. Curve block range image (OSU database). The second image shows segmentation result using canny operator.

Similar to image processing, existing approaches can be categorized in region-based and edge based techniques. Region based approaches group range pixels into connected regions using some homogeneity measure. For each region, an approximating surface model is computed. Different range image segmentation algorithms based on region growing were analyzed systematically in [Hoover et al, 1996]. There the authors also conclude that range image segmentation is still not really a solved problem even for simple industrial scenes containing polyhedral objects. More recent publications are e.g. given in [Marchall et al, 2001; Melkemi & Sapidis, 2002]. Range data is usually well suited for the extraction of smooth or planar surface patches, while the accuracy of directly extracted edges is limited. This results from the fact that range measurement is usually noisy at such discontinuities mainly due to multipath effects. For this reason only a few segmentation algorithms use edge based techniques [Sze et al, 1998; Vitulano & Maniscalco, 2004; Katsoulas & Werber, 2004]. Most of these approaches are again focused on simple polyhedral objects and are limited to the detection of specific structures such as straight lines or circles.

While in the past range data collection was mainly applied for industrial scenes captured at close distances, nowadays long-range laser scanners either terrestrial or airborne are available for many users. By these means detailed data sets of complex outdoor scenes are collected, which pose much more serious challenges for range image analysis than the traditional polyhedral world. The difficulties result from the fact that range data of natural scenes are relatively noisy. These measurement errors affect the approximation of the surfaces during segmentation. In addition, the natural scenes are complex since lots of individual objects or irregular surfaces occur. For segmentation of this type of data [Sappa et al, 2001] propose a two-step approach. The first step generates a binary edge map based on a scan line approximation technique as e.g. proposed

* Corresponding author

by [Jiang & Bunke, 1999]. The second step aims on contour extraction by a weighted graph. A minimum spanning tree (MST) is computed to obtain the shortest path, which links all the edge points. One of the main drawbacks of this algorithm is the fact that during the MST filtering many edges are eliminated. Recently [Han et al, 2004] presented a stochastic jump-diffusion algorithm for the segmentation of range images in a Bayesian framework. The algorithm can be used for processing of complex real-world scenes. Although it is considered as the most advanced algorithm for complex scene segmentation, some drawbacks such as computational complexity and the large number of required parameters are still mentioned. In addition, suitable a priori assumptions are required.

Thus, some existing algorithms are limited to high quality range images and will fail in the presence of noise. Others are complicated and have a large numbers of parameters while generic and efficient edge detectors for range images are still missing. This was our motivation for the development of an edge detection algorithm for range images. Detailed presentation of the segmentation algorithm is discussed in section 2. Section 3 discuses the characteristics and the performance of the algorithm.

2. ALGORITHM DESCRIPTION

2.1 Methodology

The approach is based on the analysis of classical differential geometry of 3D surfaces. In our algorithm, the distinguished points, which will comprise the edges within the range image, are extracted by the spatial analysis of the numerical description of the mean curvature values. For this purpose, the surface is locally approximated by an analytic representation. The different properties of the patch at the respective points of interest are then calculated analytically. In order to benefit from the behaviour of the mean curvature at edges, the algorithm detects local maxima or zero crossings in the range image. Further processing steps like a multi-scale edge detection and a subsequent skeletonization are used to increase the reliability and accuracy during the edge detection and localization.

2.2 Mathematical Properties of Mean Curvature Values

In general, successful segmentation requires an appropriate surface description. This description should be rich, so that matches of similar elements can be detected, stable so that local changes do not radically alter the descriptions, and it should have a local support so that the visible objects can be easily identified. These characteristics are provided by the mathematical properties of the mean curvature, which is closely related to the first variation of a surface area. Unlike the Gaussian curvature, the mean curvature depends on the embedding, for instance, a cylinder and a plane are locally isometric but the mean curvature of a plane is zero while that for a cylinder is non-zero. Mean curvature is invariant to arbitrary rotations and translation of surface, which is important for surface shape characterization. Since mean curvature is the average of the principal curvatures, it is slightly less sensitive to noise during numerical computations. Due to these characteristics, mean curvature values can provide stable and useful measures for detecting surface features in range and intensity images.

Several techniques are known for the efficient estimation of the mean curvature. The frequently applied analytical methods fit a surface in a local neighbourhood of the point of interest.This surface approximation is then used to compute the partial derivatives needed to calculate the curvature values. As an example [Besl & Jain, 1988] proposed an analytical technique for estimating the mean and Gaussian curvature. The advantage of this approach is its flexibility to estimate the curvature values at multiple scales, and the efficient computation of the values by optimized convolution operations. For these reasons, the estimation of the mean curvature values in our algorithm is also based on a modification of this approach. It can be summarized as follows: For a given odd $N \times N$ window, each data point is associated with a position (u, v) from the set $U \times U$ where

$$U = \{-(N-1)/2, ..., -1, 0, 1, ..., (N-1)/2\}$$

The local biquadratic surface fitting capability is provided using the following discrete orthogonal polynomials:

$\emptyset_0(u)=1,\ \emptyset 1(u)=u,\ \emptyset_2(u)=(u^2 - M(M+1)/3);\ M=(N-1)/2$

To estimate the first and second partial derivatives, an orthogonal set of $d_i(u)$ functions using the normalized versions of the orthogonal polynomials $\emptyset_i(u)$ is used:

$$\vec{d}_i(u) = \frac{\emptyset_i(u)}{P_i(M)} : P_0(M) = N, P_1(M) = \frac{2}{3}M^3 + M^2 + \frac{1}{3}M.$$
$$P_2(M) = \frac{8}{45}M^5 + \frac{4}{9}M^4 + \frac{2}{9}M^2 - \frac{1}{9}M^2 - \frac{1}{15}M.$$

Since the discrete orthogonal quadratic polynomials over the 2D window are separable in u and v, partial derivative estimates can be computed using separable convolution operators. These derivatives estimates can then be plugged into the equation for mean curvature. The equally weighted least squares derivative estimation window operators are then given by:

$$[D_u] = \vec{d}_0\vec{d}_1^T, [D_v] = \vec{d}_1\vec{d}_0^T, [D_{uu}] = \vec{d}_0\vec{d}_2^T, [D_{vv}] = \vec{d}_2\vec{d}_0^T, [D_{uv}] = \vec{d}_1\vec{d}_1^T$$

$\tilde{g}(i,j)$ represents the noisy, quantized discretely sampled version of a piecewise-smooth graph surface. Then the partial derivative estimate images are computed via appropriate 2D image convolutions.

$$\bar{g}_u(i,j) = D_u \otimes \tilde{g}(i,j),\ \bar{g}_v(i,j) = D_v \otimes \tilde{g}(i,j),\ \bar{g}_{uu}(i,j) = D_{uu} \otimes \tilde{g}(i,j)$$
$$\bar{g}_{uv}(i,j) = D_{vv} \otimes \tilde{g}(i,j),\ \bar{g}_{uv}(i,j) = D_{uv} \otimes \tilde{g}(i,j)$$

The mean curvature is then computed using the partial derivatives estimates as the following:

$$H(i,j) = \frac{(1+\bar{g}_v^2(i,j))\,\bar{g}_{uu}(i,j) + (1+\bar{g}_u^2(i,j))\,\bar{g}_{vv}(i,j) - 2\bar{g}_u(i,j)\,\bar{g}_v(i,j)\,\bar{g}_{uv}(i,j)}{2(\sqrt{1+\bar{g}_u^2(i,j)+\bar{g}_v^2(i,j)})^3}$$

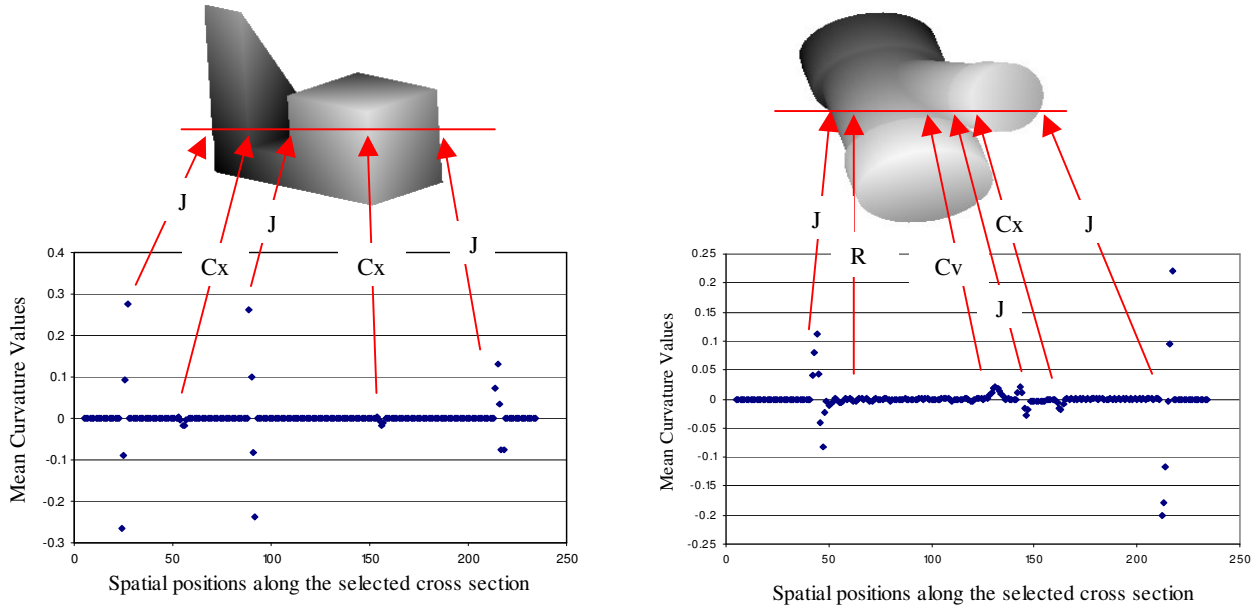

Figure 2. Spatial distribution of the mean curvature values for block and wye range image (OSU database).

2.3 Mean Curvature Spatial Analysis

The behaviour of the mean curvature for specific object properties can be demonstrated well by the filter results for synthetic range images. Thus the mean curvature was computed for range images of a block and a wye, which are depicted in Figure 1. The curvature values were then extracted at the horizontal profile represented by the line overlaid to the respective range image. From the analysis of these curvature values as they are depicted in the bottom of Figure 1 one can conclude the following:

a) For jump edge boundaries (J) where surface depths are discontinuous, the mean curvature exhibits a zero crossing. Two distinct peaks of opposite algebraic sign are clearly visible in the profile of computed curvature values.

b) For crease edges (C) at discontinuities in the surface normal direction, the curvature response is a smooth peak. Concave (Cv) and convex (Cx) edges can be discriminated by the different algebraic sign of the curvature values. The exact position of a convex crease edge is defined by the maximum curvature value, while the concave crease edge is given at a minimum.

c) At ridges (R) the mean curvature also indicates a change in the orientation of the surface normal, however, the response is smaller compared to crease edges.

d) Compared to crease edges, the values of the mean curvature are larger at jump edges. Their value mainly depends on the magnitude of the depth discontinuity.

e) Compared to crease edges, the values of the mean curvature are larger at jump edges. Their value mainly depends on the magnitude of the depth discontinuity.

f) For jump edges, the exact position is defined at a zero crossing between two peaks of the mean curvatures, whereas for both crease and ridge edges the true edge is given by the maximum and minimum peak values.

After computation of the mean curvature values $H(x,y)$ a pixel represents an edge location $\{(x,y): E(x,y)=1\}$ if the value of the gradient exceeds some threshold. Thus:

$$E(x,y)=\begin{cases}1 \; if \; \| H \| > T \; for \; some \; threshold \; T \\ 0 \; otherwise\end{cases}$$

In order to locate the position of crease, ridge and step edges, zero crossings as well as smooth peak values are searched within the computed mean curvature values during the edge detection process.

2.4 Multi-Mask Approach

Of course the effectiveness of edge detection is related to the signal-noise ratio of the data. Small-mask operators can detect fine details within range images but are sensitive against noise. In contrast, the mean curvature can be estimated more reliable using larger mask sizes of the filter operator. However, in this configuration a number of edges cannot be detected. This is especially a problem for closely neighboured edges e.g. at intersections. This is clearly visible in Figure 3a, where the red arrows mark missing edge pixels.

Since no single edge operator performs optimal for all scales, a compromise between edge localization and noise sensitivity is aspired by a multi-mask approach. By these means the missing edges are recovered correctly, as it is visible in Figure 3b. Such multi-scale approaches apply different sizes of edge operators on an image, thus different descriptions are generated where new extreme points may appear. Since the width of an edge will expand as the scale increases, a thinning process is performed to yield one-pixel wide edges. The result of this skeletonization is depicted in figure 3c.

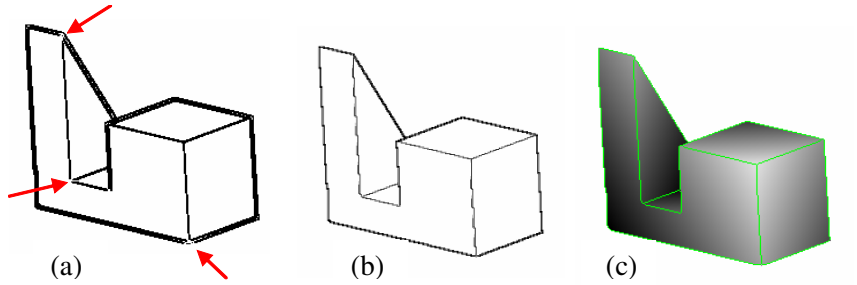

Figure 3. a) Depth and discontinuites detection using mask size 5, the red arrows show the missing parts in the junction and the corners of the object. b) Handling the junction problems using different scale threshold parameters. c) Segmentation result after thinning process to yield one pixel wide edge.

3. ALGORITHM CHARACTERISTICS

Good edge detection requires an operator, which is designed to fit the nature of a specific image. Additionally, some other characteristics of the proposed edge detector related to the nature and properties of the mean curvature will be discussed in the following.

3.1 Crease-step edge Classification

As it was already discussed in section 3, the value of the mean curvature is smaller for crease edges than for jump edges. Based on this definition, the edge types of an object can be classified easily by applying different threshold values. Low threshold values are used to detect the small peaks of crease edges while larger values can be used for step edge detection. The example of a curve block in Figure 4 demonstrates this ability of our algorithm to reliably characterize these edge types.

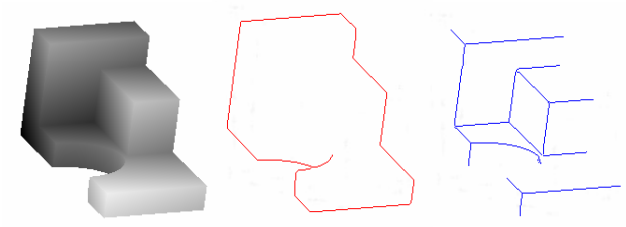

Figure 4. Curve block segmentation using different thresholds to detect step edges (red) and crease edges (blue).

3.2 Pose Independent

Range image object recognition usually decomposes into surface recognition problem, which is in turn relies on surface characterization. Segmentation process depends mainly on those characteristics. Viewpoint invariance is a desirable property for any surface characteristics derived from discrete image data. A quantity is invariant with respect to a group of transformations if those transformations do not change its value. Mean curvature value is invariant to arbitrary rotations and translations of the surface. Thus, we can expect that the algorithm can reliably detect the edges independent of the pose of the object. The performance of our technique for curvature estimation and edge detection is tested using range images with different poses. It was found that the algorithm could find the edges in all object directions using the same threshold value. The result does not affected by the arbitrary direction and rotation of the surfaces. Examples are shown in figure 5 for the block range images.

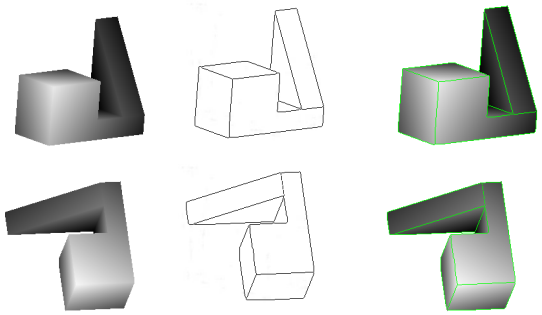

Figure 5. Block collection segmentation with different poses

3.3 Free Form Objects

A free form surface has a well-defined surface normal that is continues almost everywhere except at the edges and cusps. Discontinuities in surface normal may be presented any where on the free form surface. Similarly, discontinuities in the surface depth may be present any where in a projection of the object. The curves that connect these points of discontinuities may meet or diverge smoothly [Dorai, 1997]. Human faces and sculptures are typical examples of free form objects. It is widely accepted in the researches that the reliable segmentation and recognition of arbitrary viewed complex curved objects is still a challenging task [Campbell, 2001]. This is because free form objects are not entirely smooth but piecewise smooth. The proposed edge detection technique has been tested when free form objects considered. Figure 6 gives examples using sculptured objects obtained from OSU database. The obtained results prove that the presented technique also can deal with this kind of objects.

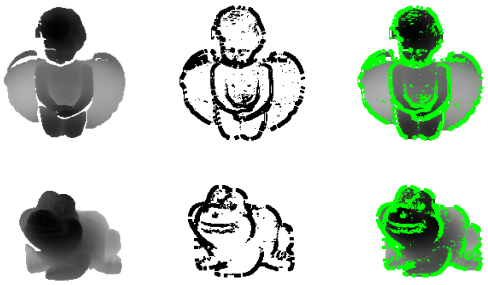

Figure 6. Segmentation results of free form objects, angle status and frog range images collected using Minolta scanner.

3.4 Real Scene Segmentation

The main challenge for most of segmentation algorithms is the robustness against noise. Thus, a number of edge detection techniques apply a smoothing process before the extraction of range changes. However, this smoothing limits the accuracy of the edge localization. In general, mean curvature is slightly less sensitive to noise in numerical computation since it is the average of the principal curvatures. In order to examine the robustness of our approach against noise, and to demonstrate its ability to deal with a variety of object surfaces, The proposed algorithm has been tested on a large number of real range images acquired by different range sensors; terrestrial and airborne laser scanners.

3.4.1 Terrestrial Laser Scanner

Figure 7 displays a range image for the 3D model of Al-Khasneh monument in ancient Petra city of Jordan. The data was collected by a Mensi GS100 laser scanner. Since such data is usually contaminated by noise, a large mask size of 11 pixels was used to allow for reliable edge detection. Figure 7b shows the binary edge map generated using the proposed segmentation algorithm. It can be noticed that the edges are thick since we have used mask size 11, which is necessary for robust estimation of the mean curvature values in such high noise images. As it is visible, most of the main features are detected. Since a large mask size was used, the edges are rather blurred. For this reason, the edges are then sketolonized by the thinning process. Figure 7c depicts the results of this process overlaid to the corresponding range image.

3.4.2 Airborne Laser Scanner

Figure 8a shows range image acquired by toposys laser scanner system for some parts of Stuttgart city, Schloss Platz area. The system provide terrain points measured at approximately one point each 1x1 m^2 with an accuracy of 0.3 m in planimetry, and 0.1 m in height. The measurements are provided along strips, which are usually processed and resampled to obtain a regular raster. The produced edge map is shown in figure 8b. Figure 8c depicts the binary edge map projected on the range image after skeletonized process.

3.5 Conclusion

The paper presents an efficient edge detection algorithm that can detect linear features in range images. The distinguished points, which will comprise the edges, depend on the spatial analysis of the numerical description of the mean curvature values. Although the central task of edge detection is to reliable detect and locate edge points, a rich description of edge points give the ability to reliably detecting and characterizing the edge types as a crease and step edges, and then go further to classify the crease edges as concave or convex types. The generality and robustness of the algorithm is illustrated on free form objects and sculptures in addition to real scene images collected with different available range sensors. Compared to known methods in literature, the algorithm exhibits the following features: computational efficiency, high accuracy in the localization of the edge points, easy to implement, and Image noise does not degenerate its performance.

Figure 7. a) Range images collected from Petra treasury (Al-Khasneh). b) Segmentation results using mask size 11. c) Edge map projected in the range image after skeletonized.

Figure 8. a) Range image for Schloss Platz area, Stuttgart city. b) Segmentation results using mask size 11. c) Edge map projected in the range image after skeletonized.

REFERENCES

Alshawabkeh, Y. & Haala N. [2005], Automatic Multi-Image Photo Texturing of Complex 3D Scenes. CIPA IAPRS Vol. 34-5/C34, pp. 68-73.

Besl, P. & Jain, R. [1988], Segmentation Through Variable-Order Surface Fitting. IEEE Transactions on Pattern Analysis and Machine Intelligence, 9(2): 167–192.

Bruni, V., Vitulano, D. & Maniscalco,U. [2004], Fast Segmentation and Modeling of Range Data Via Steerable Pyramid and Superquadrics. The 12-th International Conference in Central Europe on Computer Graphics, Visualization and Computer Vision'2004, WSCG 2004, University of West Bohemia, Czech Republic.

Canny, J. [1986], A Computational Approach to Edge Detection, IEEE Transactions on Pattern Analysis and Machine Intelligence, Vol. 8, No. 6, Nov.

Chen, C. & Stamos, I. [2007], Range Image Segmentation for Modeling and Object Detection in Urban Scenes. The 6th International Conference on 3-D Digital Imaging and Modeling, Montreal, Canada, August 21-23.

Christy, S. & Horaud, R. [1996], Iterative Pose Computation from Line Correspondences. Computer Vision and Image Understanding Vol. 73, No. 1, January, pp. 137–144.

Djebali, M., Melkemi, M. & Sapidis, N. [2002], "Range-Image Segmentation and Model Reconstruction Based on a Fit-and-Merge Strategy," ACM Symposium on Solid Modeling and Applications, pp.127-138.

Dorai, C. [1997], COSMOS—A Representation Scheme for 3D Free-Form Objects IEEE Transactions on Pattern Analysis and Machine Intelligence. Vol PAMI-19, no 10.

Gächter, S. [2005], Results on range image segmentation for service robots. Technical Report. Switzerland.

Gachter, S., Nguyen, V. & Siegwart, R. [2006], Results on Range Image Segmentation for Service Robots. IEEE International Conference on Computer Vision Systems. 2006 ICVS.

Han, F., Tu, Z. & Zhu, S. [2004], Range image segmentation by an efficient jump-diffusion method. In IEEE Trans. On Pattern Analysis and Machine Intelligence.Vol.26/9. pp.1138-1153.

Haralick, R., Lee, C., Ottenberg, K. & Nolle, M. [1994], Review and analysis of solutions of the 3-point perspective pose estimation problem. IJCV 13(3), pp. 331–356.

Hoover, A., Jean-Baptiste, G. & Jiang, X. [1996], An Experimental Comparison of Range Image Segmentation Algorithms. IEEE Transactions on Pattern Analysis and Machine Intelligence, 18(7): p. 673-689.

Jiang, X. & Bunke, H. [1999], Edge detection in range images based on scan line approximation. Computer Vision and Image Understanding: CVIU, 73(2): 183–199.

Katsoulas, D. & Werber, A. [2004], Edge Detection in Range Images of Piled Box-like Objects. 17th International Conference on Pattern Recognition (ICPR 2004), 4-Volume Set, Cambridge, UK. IEEE Computer Society, ISBN 0-7695-2128-2.pp 80-84.

Marshall, D., Lukacs, G. & Martin, R. [2001], Robust segmentation of primitives from range data in the presence of geometric degeneracy; IEEE Trans. Pattern Analysis and Machine Intelligence 23(3), 304-314.

Ohio State University range Image Collection, http://sampl.ece.ohio-state.edu/data/.

Palmer, P., Dabis, H. & Kittler, J. [1996] A performance measure for boundary detection algorithms. CVGIP: Image Understanding, 63(3): 476-494.

Sappa, A. & Devy, M. [2001], “Fast Range Image Segmentation by an Edge Detection Strategy,” Proc. IEEE Conf. 3D Digital Imaging and Modeling, pp. 292-299.

Sze, C., Liao, H., Hung, H., Fan, K. & Hsieh, J. [1998], “Multiscale edge detection on range images via normal changes,” IEEE Transition. Circuits System. II, vol. 45, pp. 1087–1092.

Yu, Y., & Ferencz, A., [2001] Extracting Objects from Range and Radiance Images. IEEE Transactions on Visualization and Computer Graphics, Vol /, No.4.